Supporting Information

Cerium-doped bimetal organic framework as a superhigh capacity cathode for rechargeable alkaline batteries†

Junpeng Li,[ab] Guobang Zhao,[a] Hongyang Zhao,[c] Ningning Zhao,[a] Miao Wang,[d] Leilei Lu,[a] Nailiang Liu,[a] Chunjie Ma,[e] Qian Zhang*[ab] and Yaping Du*[b]

[a.] J. Li, G. Zhao, N. Zhao, Leilei Lu and N. Liu

Department of Applied Chemistry, Xi'an University of Technology.

Xi'an, Shaanxi 710048, China.

Prof. Q. Zhang

State Key Laboratory of Eco-hydraulics in Northwest Arid Region, Department of Applied Chemistry, Xi'an University of Technology.

Xi'an, Shaanxi 710048, China.

E-mail: qzh@xaut.edu.cn (Q. Zhang)

J. Li and Q. Zhang are also visiting scholars at Rare Earth Center (see below)

[b.] Prof. Y. Du

Tianjin Key Lab for Rare Earth Materials and Applications, Center for Rare Earth and Inorganic Functional Materials, School of Materials Science and Engineering & National Institute for Advanced Materials, Nankai University.

Tianjin 300350, China.

E-mail: ypdu@nankai.edu.cn (Y. Du)

[c.] H. Zhao

Frontier Institute of Science and Technology, Xi'an Jiaotong University.

Xi'an, Shaanxi 710054, China.

[d.] M. Wang

Shaanxi Research Institute of Textile Accessories

Xianyang, 712000, China.

[e.] C. Ma

Shaanxi J&R Optimum Energy Co., Ltd.

Qingyang Building, Tsinghua Science Park, High-Tech Industries Development Zone, Xi'an 710075, P. R. China.

† Electronic supplementary information (ESI) available. See DOI: xxxxx

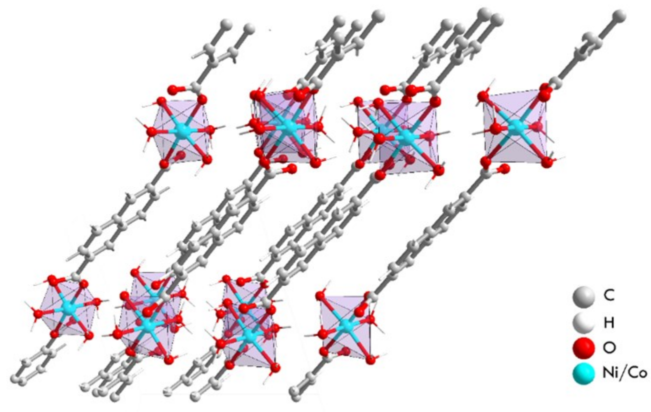

Figure. S1 Crystal structure of NiCo-MOF

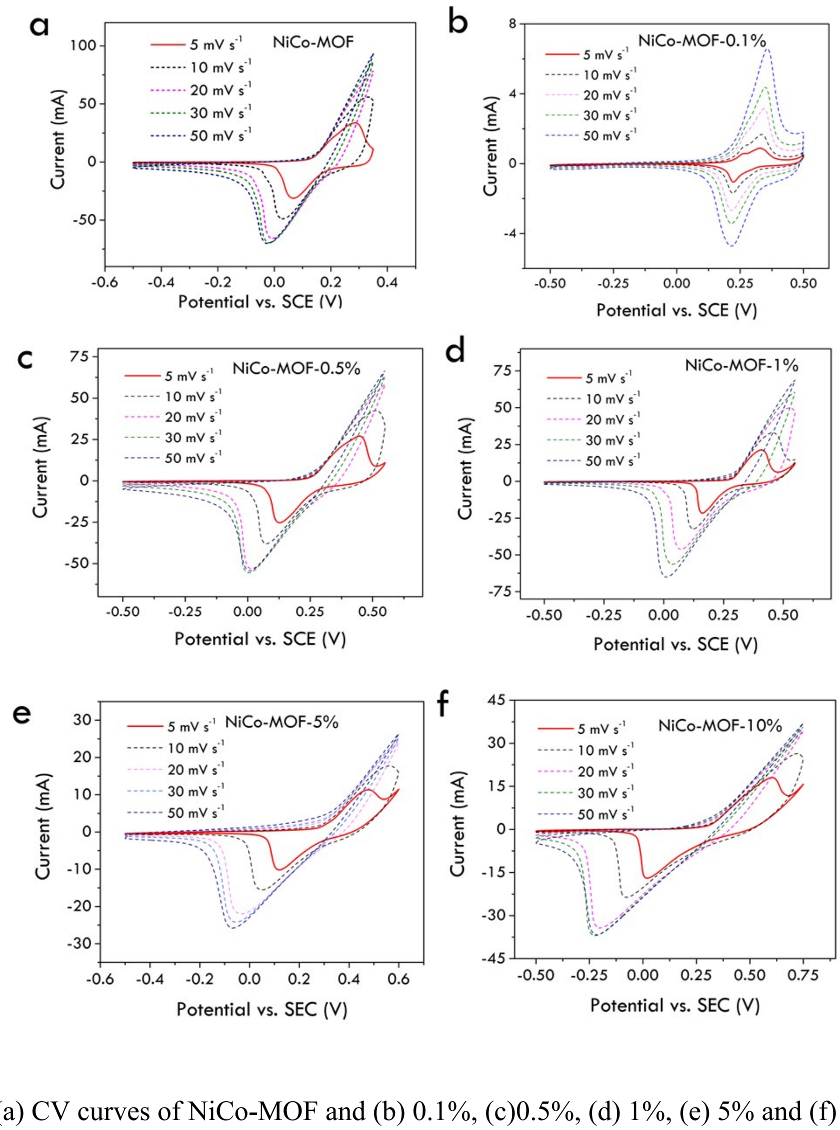

Figure S2. (a) CV curves of NiCo-MOF and (b) 0.1%, (c)0.5%, (d) 1%, (e) 5% and (f) 10% Ce doping NiCo-MOF. Scan rates ranging from 5 mV s^{-1} to 50 mV s^{-1}.

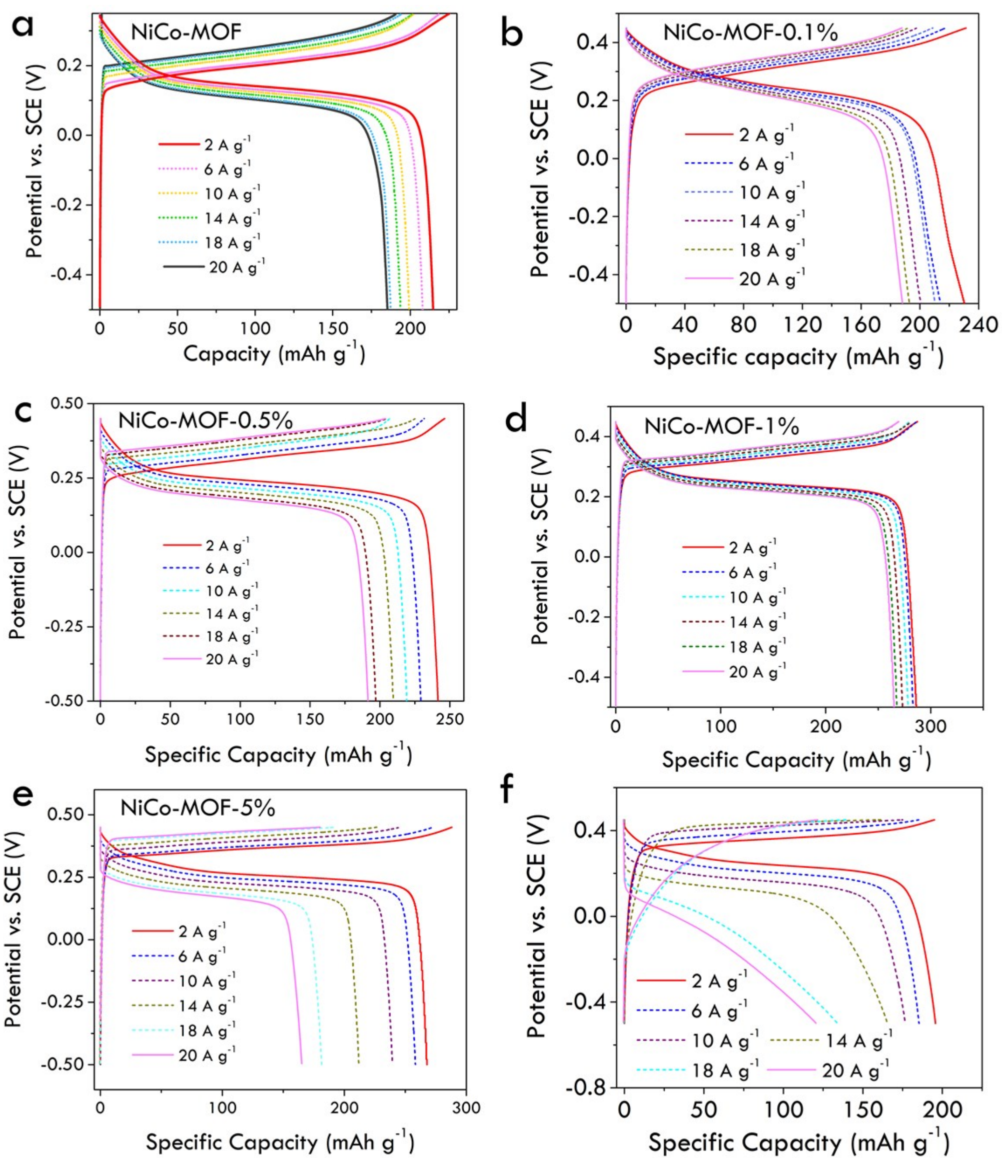

Figure S3. Charge and discharge profiles of (a) NiCo-MOF, (b) 0.1% Ce doping NiCo-MOF, (c) 0.5% Ce doping NiCo-MOF, (d) 1% Ce doping NiCo-MOF, (e) 5% Ce doping NiCo-MOF and (f) 10% Ce doping NiCo-MOF at current densities of 2 A g^{-1}, 6 A g^{-1}, 10A g^{-1}, 14 A g^{-1}, 18 A g^{-1} and 20 A g^{-1}.

Table S1. Potential and capacity performance

Active materials	*Potential vs. SCE at 2 A g^{-1} (V)	Capacity at 2 A g^{-1}	Capacity at 20 A g^{-1}	Rate capacity retention
NiCo-MOF	0.139	215	185	86%
NiCo-MOF-0.1%	0.236	230	188	82%
NiCo-MOF-0.5%	0.237	241	191	79%
NiCo-MOF-1%	0.244	286	265	93%
NiCo-MOF-5%	0.257	268	165	62%
NiCo-MOF-10%	0.243	195	120	62%

* Discharge potential at 50% discharge capacity

Discharge capacity of NiCo-MOF and NiCo-MOFs with various Ce doping at current densities from 2 A g^{-1} to 20 A g^{-1} was shown in Figure S3. The data in Table S1 were obtained from Figure S3, indicating Ce benefited discharge voltage with increasing doping amount. NiCo-MOF with 1% Ce doping performed higher capacity and rate capacity retention (93% from 2 A g^{-1} to 20 A g^{-1}). Obviously NiCo-MOF with 1% Ce doping outperforms others.

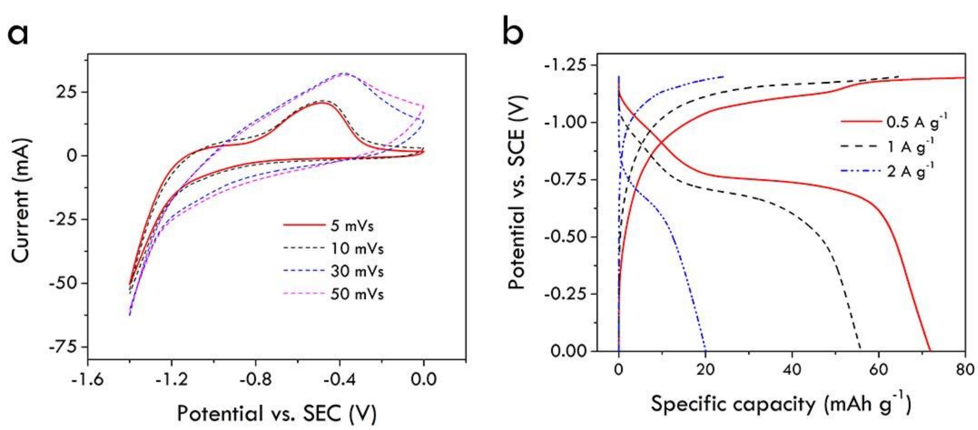

Figure S4. Electrochemical performance of Fe_2O_3 anode. (a) CV plots at scan rates from 5 mV s^{-1} to 50 mV s^{-1}. (b) Charge and discharge curves from 0 V to -1.2 V at current densities of 0.5 A g^{-1}, 1 A g^{-1} and 2 A g^{-1}.

CV curves at scan rates of 5 mV s^{-1}, 10 mV s^{-1}, 30mV s^{-1} and 50 mV s^{-1} were available in Figure S4(a). The charge and discharge profiles in Figure S4(b) indicate the capacity was 72 mAh g^{-1}, 56 mAh g^{-1} and 20 mAh g^{-1}, at 0.5 A g^{-1}, 1 A g^{-1} and 2 A g^{-1}, respectively. According to a previous report the charge-discharge mechanism is proposed as follows:[1]

Fe_2O_3 anode was activated, $Fe_2O_3 + H_2O \longrightarrow 2FeOOH$ (1)

Discharge process: $FeOOH + H_2O + e^- \longrightarrow Fe(OH)_2 + OH^-$ (2)

Charge process: $Fe(OH)_2 + OH^- \longrightarrow FeOOH + H_2O + e^-$ (3)

Table. S2 Performance comparison of the aqueous batteries with NiCo-MOF-1%/Fe_2O_3 battery

Cathode	Anode	Energy density (Wh kg^{-1})	Power density (kW kg^{-1})	Reference
NiCo-MOF-1%	Fe_2O_3	150	0.78	This work
NiCo-MOF-1%	Fe_2O_3	102	3.75	This work
$NiCo_2O_4$	Bi	85.8	1.0	2
Co-doped $Ni(OH)_2$	Zn	148	1.7	3
$LiMn_2O_4$	$LiTi_2(PO_4)_3$	60	0.1	4
$LiNi_{0.5}Mn_{1.5}O_4$	Mo_6S_8	126	N/A	5
Ni/NiO	Bi/Carbon	105	N/A	6
Mn doping $Ni(OH)_2$	Active carbon/RGO	51.5	0.4	7
Co-Cd selenide	Fe	57.6	10.9	8
$Ni(OH)_2$	Fe_2O_3	100.7	0.287	9
$Ni(OH)_2$	Active carbon	35.7	0.49	10

The energy density (*E*) and power density (*P*) based on active materials of cathode and anodes electrodes were calculated by Eq (1).[11] The full cell exhibited a high energy density of 150 Wh kg^{-1} at the lowest power density of 0.78 kW kg^{-1}, while it can hold 102 Wh kg^{-1} at 3.75 kW kg^{-1}.

$$E = \int_0^t \frac{I\Delta U}{m} dt \qquad P = \frac{1}{t}\int_0^t \frac{I\Delta U}{m} dt \tag{1}$$

Where I is the constant discharge current, t is discharge time, ΔU is discharge voltage range, m is the mass of active materials on cathode and anode electrodes.

References:

1. K. A. Owusu, L. Qu, J. Li, Z. Wang, K. Zhao, C. Yang, K. M. Hercule, C. Lin, C. Shi, Q. Wei, L. Zhou and L. Mai, *Nat. Commun.*, 2017, **8**, 14264.
2. Y. Zeng, Z. Lin, Y. Meng, Y. Wang, M. Yu, X. Lu and Y. Tong, *Adv. Mater.*, 2016, **28**, 9188.
3. C. Xu, J. Liao, C. Yang, R. Wang, D. Wu, P. Zou, Z. Lin, B. Li, F. Kang and C. Wong, *Nano Energy*, 2016, **30**, 900.
4. J. Y. Luo and Y. Y. Xia, *Adv. Funct. Mater.*, 2007, **17**, 3877.
5. F. Wang, L. Suo, Y. Liang, C. Yang, F. Han, T. Gao, W. Sun and C. Wang, *Adv. Energy Mater.*, 2017, **7**, 1600922.
6. Y. Zeng, Z. Lin, Z. Wang, M. Wu, Y. Tong and X. Lu, *Adv. Mater.*, 2018, **30**, 1707290.
7. L. Ye, Y. Zhou, Z. Bao, Y. Zhao, Y. Zou, L. Zhao and Q. Jiang, *J. Mater. Chem. A,* 2018, **6**, 19020.
8. Z. Zhai, K. Huang and X. Wu, *Nano Energy*, 2018, **47**, 89.
9. J. Liu, M. Chen, L. Zhang, J. Jiang, J. Yan, Y. Huang, J. Lin, H. J. Fan and Z. X. Shen, *Nano Lett.*, 2014, **14**, 7180.
10. H. Li, M. Yu, F. Wang, P. Liu, Y. Liang, J. Xiao, C. Wang, Y. Tong and G. Yang, *Nat. Commun.*, 2013, **4**, 1.
11. H. Lai, Q. Wu, J. Zhao, L. Shang, H. Li, R. Che, Z. Lyu, J. Xiong, L. Yang and X. Wang, *Energy Environ. Sci.*, 2016, **9**, 2053.